Effect of Welding Parameters on Mechanical Properties of Dissimilar Friction Stir Lap Welds of AA5052 and AISI 1010

L. N. Tufaro and H. G. Svoboda

Abstract Friction stir lap welding (FSLW) is a solid-state welding process which allows joining of similar and dissimilar materials. Welding of dissimilar materials involving aluminium alloys and steels are a current requirement for several industries, mainly for automotive and transportation. Al/steel joints presents several challenges, due to its different physical properties and the formation of intermetallic compounds. FSLW is a particularly interesting welding technique for these joints, especially for thin sheets. Nevertheless, there is lack of information about its application. The welding parameters affect the microstructural evolution, the material flow, defects level, distortions, etc. The aim of this work is to analyse the effect of the travel speed on the mechanical properties of friction stir lap welds of AA5052 aluminium alloy and AISI 1010 low carbon steel in thin sheets (1 and 0.8 mm, respectively). Dissimilar friction stir lap welds of these materials were produced using a tool made of H13 tool steel. Diverse travel speeds were analysed (98, 146 and 206 mm/min). Macrostructure examination, microhardness profiles and maps were performed in the weld cross section. Lap shear tests were conducted, and the fracture surfaces of tested samples were analysed. The maximum load per width unit increased linearly with travel speed, reaching 190 N/mm and a joint efficiency of 73%, and is controlled by the amount of steel inclusions in the aluminium plate through, which decreases with travel speed.

Keywords Friction stir lap welding (FSLW) · Al to steel dissimilar joints · Travel speed · Hook · Steel inclusions

L. N. Tufaro
Centro de Investigación y Desarrollo en Mecánica, Instituto Nacional de Tecnología Industrial, Av. Gral. Paz 5445, B1650WAB San Martín, Argentina
e-mail: ltufaro@inti.gob.ar

L. N. Tufaro · H. G. Svoboda (✉)
INTECIN, Universidad de Buenos Aires, Paseo Colón 850, C1127AAR Buenos Aires, Argentina
e-mail: hsvobod@fi.uba.ar

H. G. Svoboda
CONICET, Godoy Cruz 2290, C1033AAJ Buenos Aires, Argentina

1 Introduction

Dissimilar joints are widely used in multi-materials structures and thin sheet overlap Aluminium to Steel joints are especially relevant in automotive industry.

Friction stir lap welding (FSLW) is a solid-state welding process which allows joining similar and dissimilar materials. The capability of FSLW for the joining of dissimilar material, such as aluminium and steel, lies in the low heat input that minimize the extent of intermetallic compound (IMC) formation during the welding process (Kumar et al. 2015; Kar et al. 2020; Sorger et al. 2017).

In friction stir welding (FSW) of steels, the most common tool materials are WC and PCBN (Mishra and Mahoney 2007), although it was reported that tool steel can be used in FSLW of Al to Steel joints when the steel is place in the bottom of the joint and the tool pin plunge in the steel is null or low (Chen et al. 2013; Kumar et al. 2015). The level of interaction between the pin and the steel sheet will affect the tool life as well as the mixing between aluminium and steel. It was reported that a slight pin penetration in the steel plate (P_P) of 0.1 mm has not produced a significant wear of the pin (Chen et al. 2013; Kumar et al. 2015). Other authors also have used some degree of pin plunge for this type of joint (Coelho et al. 2008; Elrefaey et al. 2005; Kar et al. 2020; Kimapong and Watanabe 2005a, b; Movahedi et al. 2011, 2012; Wan and Huang 2017).

The pin plunge into the steel sheet led to the formation of a steel hook within the aluminium alloy. This hook can affect the mechanical properties of the welded joint. Two geometrical effects can be pointed out related to the hook formation. One is related to the reduction in the effective thickness of the aluminium alloy sheet (Sorger et al. 2017). Other authors have reported some beneficial effect related to the mechanical locking produced by the steel flow into the Al sheet (Movahedi et al. 2011, 2012).

In general, it seems that some degree of interaction between the pin and the steel sheet is needed to perform the FSLW of aluminium to steel Nevertheless, Chen et al. (2013) have reported that the optimal condition corresponds with a null P_P but with the pin close to the steel plate in order to produce a continued interface intermetallic layer which is the condition for a continued metallurgical bonding.

The mechanical properties of this type of joints are a key aspect for its application. Lap shear test is usually used to evaluate the strength and integrity of the joint. The fracture mode in this test depends on the aluminium/steel interface integrity and local materials strengths and thicknesses. The fracture can produce through the aluminium/steel interface in a shear mode (Chen et al. 2013, Kar et al. 2020, Kimapong and Watanabe 2005a, b, Movahedi et al. 2011, Movahedi et al. 2012, Wan and Huang 2017), or through the thickness of one of the base materials in a tensile mode (Coelho et al. 2008; Kimapong and Watanabe 2005a; Movahedi et al. 2011, 2012). For the first fracture type, it was found that an increase in travel speed (U) and a decrease in rotational speed (ω) produce a reduction of the heat input, resulting in a thinner IMC layer and in a higher a fracture load (Kimapong and Watanabe 2005a; Wan and Huang 2017). Kimapong and Watanabe reported that a variation in

ω can change the fracture mode, obtaining a fracture located in the aluminium for lower ω with higher fracture loads, while the fracture was located at the interface for higher ω, with lower loads. They also reported that an excessively high U produces a joint with incompletely welded interface, reducing the fracture load (Kimapong and Watanabe 2005a, b).

Movahedi et al. found that a variation in U can also change the fracture mode. They obtained joints with cavities at the interface for higher U, resulting in a fracture located in the interface with lower fracture loads, while defect free joints were produced for lower U, presenting a fracture at the steel sheet with higher fracture loads (Movahedi et al. 2011, 2012).

The effect of other welding parameters was also analysed. An increase in P_P, pin diameter and tool tilt angle produce a reduction in fracture load, which is related with the IMC layer thickness at the interface and defect generation (Kimapong and Watanabe 2005a, b). Not only the thickness of the IMC layer affects the fracture load, but it was also found that grain refinement of the IMC layer highly enhances the joint strength by increasing the fracture toughness of the brittle IMC layer (Beygi et al. 2021).

Coelho et al. (2008) studied FSLW of AA6181-T4 alloy and HC340LA, obtaining a fracture through the aluminium sheet thickness, suggesting that the amount and the size of the steel inclusions in the Al sheet apparently determine the mechanical properties of the joint.

Despite that FSLW of dissimilar joints of aluminium and steel was subject of different works in the last years, there is still a lack of comprehension of the effect of welding conditions and tool geometries on the mechanical behaviour of the joints, especially for thin sheets.

The objectives of this work were to develop a welding procedure for dissimilar AA5052-H32 aluminium alloy and AISI 1010 carbon steel by FSLW in thin sheets and to analyse the effect of the travel speed on the mechanical strength of friction stir lap welds of AA5052 and AISI 1010.

2 Materials and Methods

Dissimilar lap welds of AA5052-H32 and AISI 1010 in thin sheets of 1 mm and 0.8 mm thickness (t), respectively, were produced by FSLW. Table 1 presents the mechanical properties of base materials used in this work.

Table 1 Mechanical properties of base materials

Material	HV (0.3 kg)	$\sigma_{0,2}$ (MPa)	σ_{UTS} (MPa)	e (%)
AA5052-H32	65	205	260	13.5
AISI 1010	95[a]	180[a]	320[a]	28[a]

[a]Minimum values
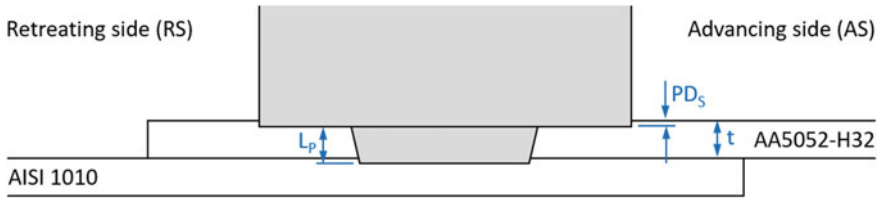
Fig. 1 Scheme of FSLW process

The test coupons were formed by samples of each sheet of 50 mm width and 125 mm long, overlapped 25 mm, as it is shown in Fig. 1. AA5052-H32 was located as the upper sheet, in the advancing side (AS), while AISI 1010 steel sheet was located as the lower one, in the retreating side (RS).

The tool was made of H13 tool steel with a concave shoulder of 12 mm in diameter and a tapered pin, with major minor diameters of 6.2 and 5.7 mm, respectively. The pin length (L_P) was 1 mm like the aluminium alloy plate t, in order to obtain a pin penetration (P_P) in the steel plate similar to the shoulder plunge depth (PD_S). The rotational speed was 680 rpm and different travel speeds (U) were analysed: 98, 146 and 206 mm/min, using this parameter for the sample identification. The tilt angle was 1.5° and the shoulder plunge depth was of the nominally of 0.1 mm.

Cross sections of welded samples were prepared for metallographic observation. Macrostructure examination was performed in order to analyse the material mixing at the aluminium/steel interface and for the measurement of dimensional characteristics of the joints (Fig. 2): welding nugget thickness corresponding to the Al sheet (t_{WN}) and hook position from the weld centreline (P_{Hook}).

The resulting underfill (h) was calculated as the difference between the WN and the parent material (PM) thicknesses (h = t − t_{WN}). Dimensional aspects specified on ISO 25392 were verify in order to analyse the qualification of the welding procedure (ISO 25239-4: 2011).

Vickers microhardness profiles (HV) were carry out along the mid-thickness line of the aluminium alloy plate with a spacing of 0.60 mm. Also, Vickers microhardness maps ($HV_{0.1}$) were performed in the aluminium plate at the hook region. The maps were centred in the mid thickness of the PM, with a horizontal and vertical spacing
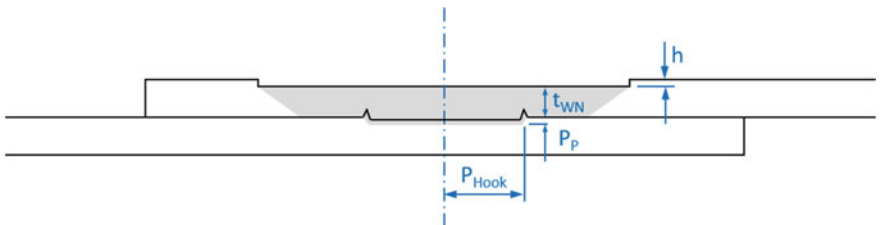
Fig. 2 Scheme of joint dimensional characteristics
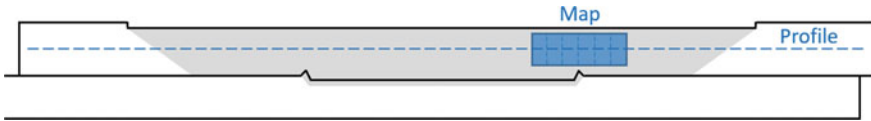
Fig. 3 Scheme of Vickers microhardness measurement locations for profiles and maps

between indentations of 0.30 mm. A scheme of the Vickers microhardness profile and map locations is shown in Fig. 3.

Two specimens from each welding condition were extracted to perform lap shear tests. Load–displacement curves were recorded obtaining the maximum load per width unit (P_{max}/w) for each case. On tested samples of each condition, longitudinal sections were prepared to microstructural examination in order to analyse the fracture location and path. Also, the fracture surface of the specimens was analysed with scanning electron microscopy (SEM) and energy dispersive X-ray spectrometry (EDS).

3 Results and Discussions

Figure 4 shows the macrographs of the weld cross section for the different welding conditions. For all cases, interaction between the aluminium and the steel was obtained. It can be seen a good aluminium/steel interface appearance without showing voids or other macrographic defects.

Geometric characteristics determined are shown in Table 2. The t_{WN} was of the order of 0.9 mm, related with an h of 0.1 mm, although for the 146 mm/min condition the t_{WN} was slightly lower. Despite of that, all the joints satisfy the acceptance limit for the underfill of the ISO 25239, which is 0.15 mm for 1 mm thickness plates (ISO 25239-4: 2011). The P_{Hook} and the extension of the aluminium/steel interface were decreased with U. The P_{Hook} is indicated with an arrow in the macrographs (Fig. 4).

Steel inclusions (SI) are observed embedded into the aluminium plate, mainly located at the hook region. The amount of SI also decreased with U. Even though the pin penetration in the steel plate has a significant impact in the material flow at the interface, the slightly variations in the pin penetration (related with the underfill) do not explain the observed changes in the material flow. In this sense, the changes in material flow can be related with the U.

From the macroscopic examination it could be said that the developed procedure showed to be adequate to achieve a suitable material mixing and could be qualify under ISO 25239, considering this standard is developed for aluminium alloys (ISO 25239–4: 2011).

Vickers microhardness profiles in the AA5052 for the three welding conditions are shown in Fig. 5 with a schematic of a weld cross section to associate the corresponding position into the weld joint.
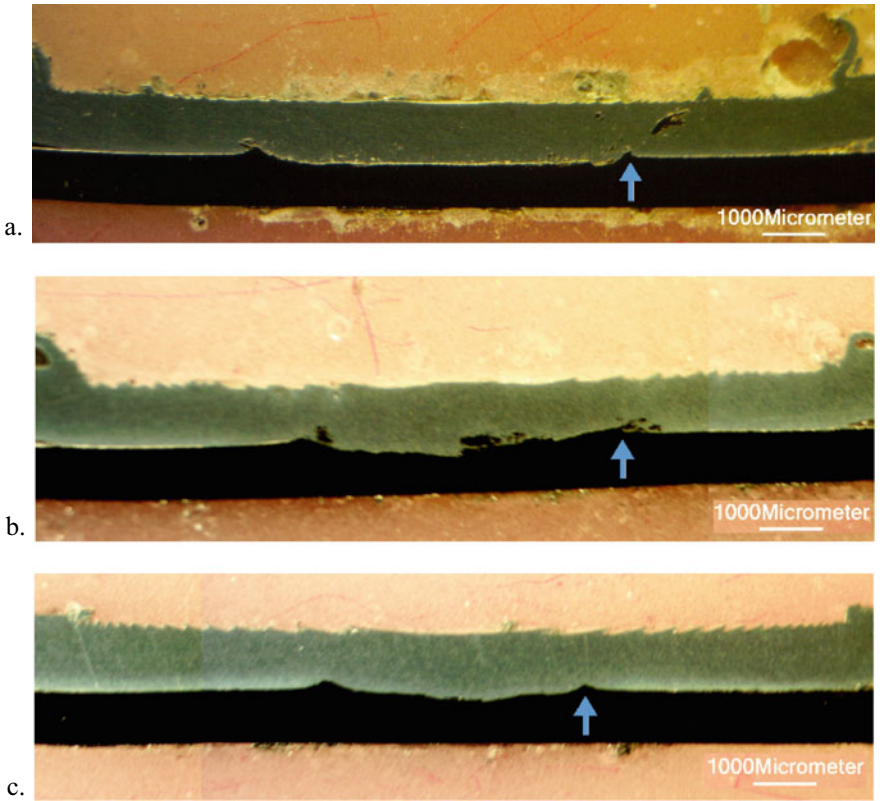
Fig. 4 Macrographs of weld cross section: a. 98, b. 146, c. 206

Table 2 WN geometric characteristics

U (mm/min)	t_{WN} (mm)	h (mm)	P_{Hook} (mm)
98	0.89	0.11	3.06
146	0.86	0.14	2.61
206	0.91	0.09	2.05

The AA5052 is a work hardened aluminium alloy with an average hardness of 75 $HV_{0.3}$. In the HAZ it can be seen a reduction in the hardness, which is related to the recovery and recrystallization due the thermal cycle experimented during the welding process. This behaviour has been reported for work hardened aluminium alloys welded by FSW (Mishra and Mahoney 2007). The hardness in the WN is relatively uniform with an average value of the order of 65 $HV_{0.3}$, similar to the obtained at the high temperature HAZ. Nevertheless, for the lower U (98 mm/min), local values over the average WN hardness were measured, which were associated

**Fig. 5** Vickers
microhardness profiles
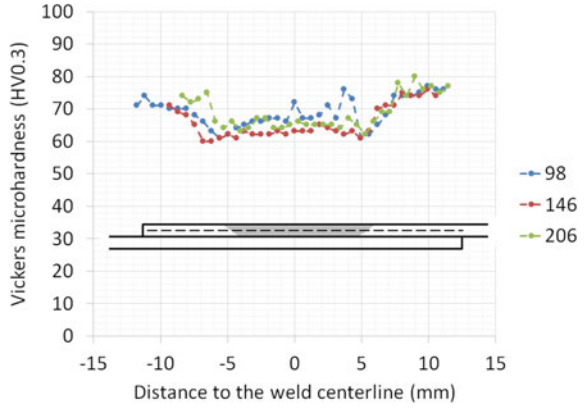
to the SI in the Al sheet. In general, there is no significant variations of the hardness
profiles with U.

Vickers microhardness maps performed in the AA5052 at the hook region for the
three welding conditions, with a black and white image of the macrograph displaying
the SI distribution in the aluminium alloy sheet, are shown in Fig. 6. The nodes of

Fig. 6 Vickers
microhardness maps
($HV_{0.1}$): **a** 98, **b** 146, **c** 206
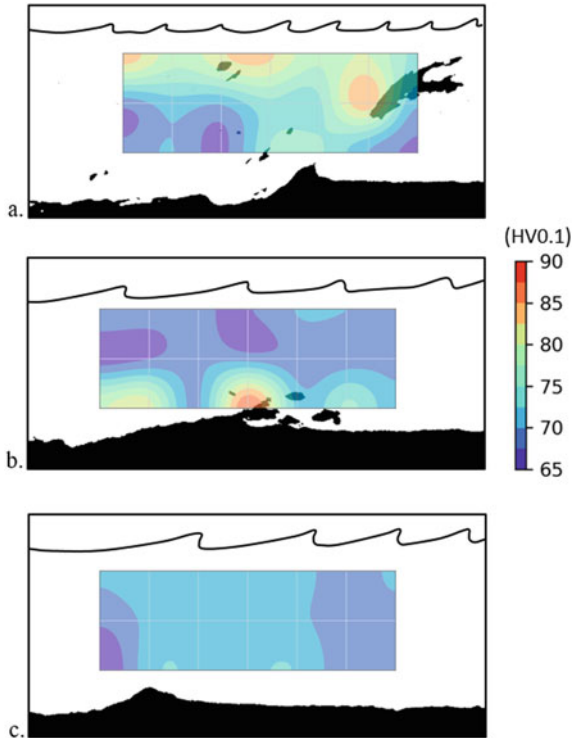
Fig. 7 Curves Load per
width unit (P/w) -
Displacement (Δl) of lap
shear tests for different U
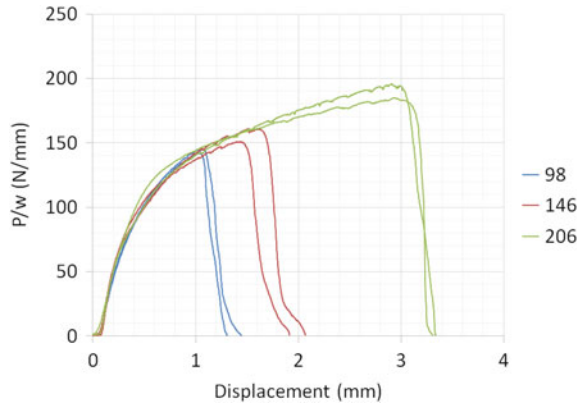
the grid of the maps are associated with the measurement positions.

The hardness maps show values from 65 to 85 $HV_{0.1}$, approximately corresponding to the Al alloy. The uniformity of the hardness in the analysed zone increased with U. The hardness peaks measured are related with the zones adjacent to the SI. In this sense, although thermal softening of the Al alloy could increase as U decreases, the presence of higher amounts of SI could explain the increase in hardness at the hook zone for lower U. For higher U the amount and size of SI decrease, explaining the higher uniformity of the hardness measured and the lower values obtained.

In Fig. 7 the Load per width unit-Displacement curves obtained from the lap shear tests are shown. The maximum load as well as the displacement at maximum load increased with travel speed. Consequently, the total area under the curve also increased with U. It can be seen the low dispersion between both test samples for each condition.

The plot of P_{max}/w vs. U as well as the equivalent joint efficiency (Ef), considering the tensile strength of the AA 5052-H32, is shown in Fig. 8.

P_{max}/w increased linearly with U, reaching an average value of 190 N/mm (for 206 mm/min). The linear correlation obtained shows a good agreement ($R^2 = 0.96$). The Ef increased from 55% up to 73% for 206 mm/min. This maximum Ef reached resulted higher than the reported ones for FSLW of dissimilar joints of work hardened aluminium alloy and steel (Sorger et al. 2017), representing a very promising result.

P_{max}/w, fracture location and mode are defined by the aluminium/steel interface integrity, local materials strengths (microhardness) and joint dimensions (local thicknesses). In all the cases, the fracture was located in the WN of the aluminium plate, presenting a tensile fracture mode, as can be seen in Fig. 9. Therefore, the strength of the interface between both plates was higher than de strength of the aluminium plate at the WN.
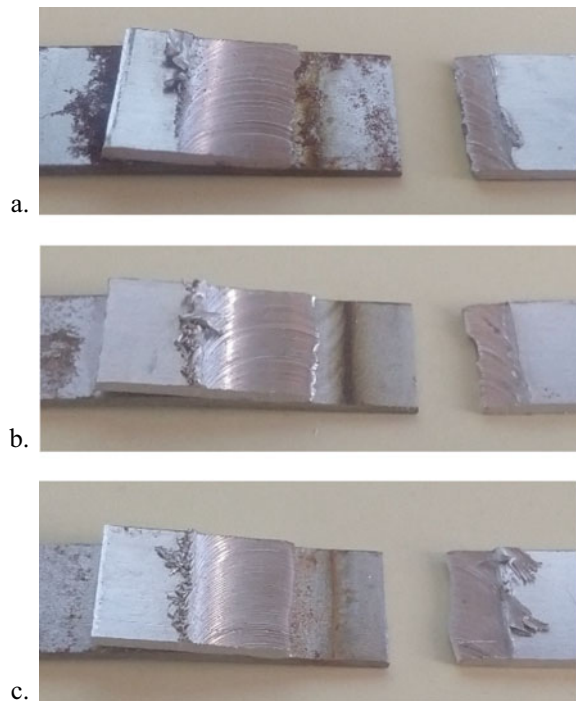
P_{max}/w for the U of 146 mm/min was below the obtained linear tendency showed in Fig. 8. This fact could be related with the slightly lower measured t_{WN} for this

**Fig. 8** Maximum load per width unit (P_{max}/w) and joint efficiency (Ef) versus travel speed (U)
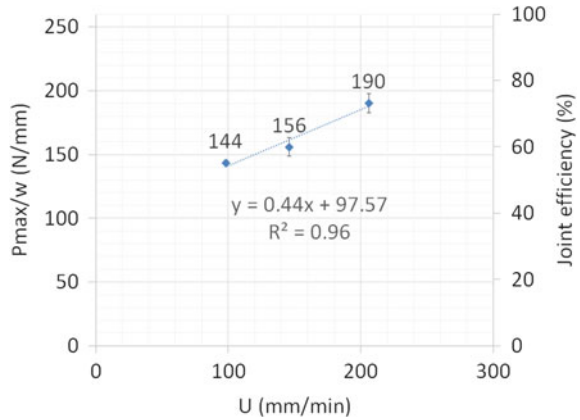
Fig. 9 Fractured lap shear test specimens: **a** 98, **b** 146, **c** 206

condition (Table 2). Despite of that, there is no significant effect of the t_{WN} of the AA5052 plate.

The hardness in the fracture location does not exhibit major variations with U, regardless the effect of the SI presence in the aluminium plate. Therefore, the P_{max}/w improvement with increasing U would be controlled by another phenomenon. In Fig. 10 are shown the macro and micrographs of lap shear test specimens, with and without etching.
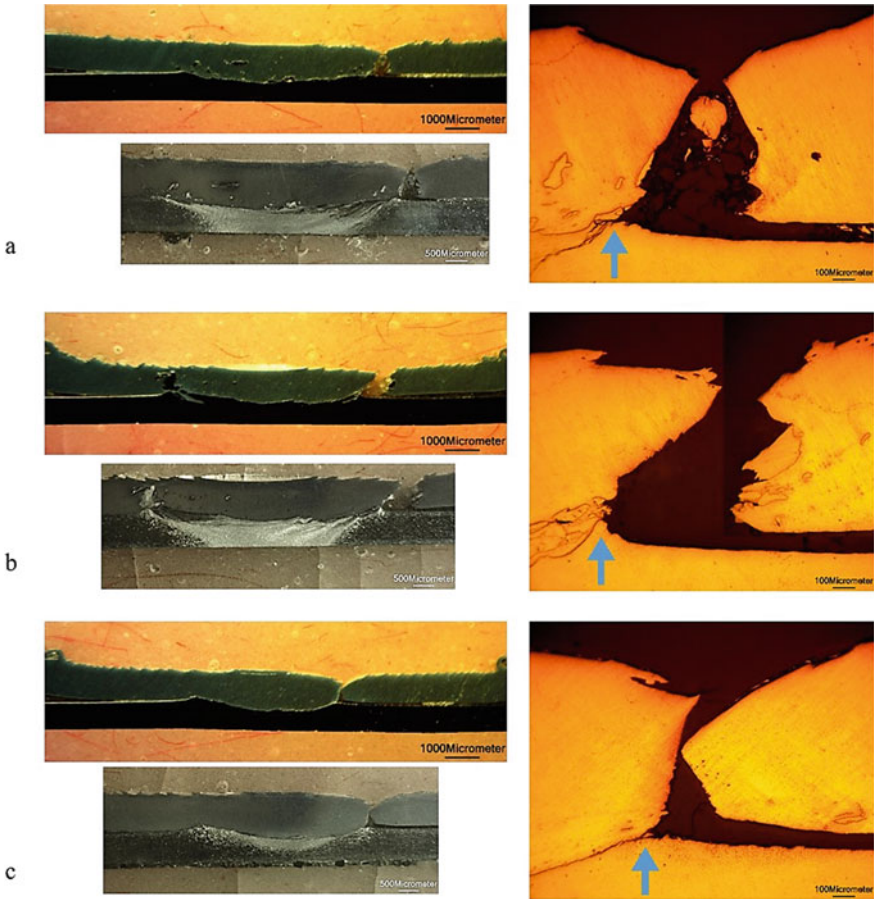
Fig. 10 Macro and micrographs of lap shear test specimens: **a** 98, **b** 146, **c** 206

For all welding conditions, the fracture initiates at the hook position (P_{Hook}), which is indicated with an arrow in the micrographs. It was reported previously the hook reduces locally the t_{WN} of the aluminium plate, promoting the fracture in this position (Sorger et al. 2017). Additionally, the fracture path is associated to the SI in the aluminium plate, which are located mainly in the hook region. As can be seen in Fig. 9a, b, the fracture propagated partially through the aluminium/SI interface, probably due to the presence of the brittle intermetallic compound (IMC) (Chen et al. 2013; Sorger et al. 2017).

For the higher U, lower amounts of SI were in the fracture path (Fig. 9c). Therefore, P_{max}/w would be controlled by the amount of SI in the aluminium sheet at the hook region in the t_{WN}, which decreased with the increase of U, producing an improvement in P_{max}/w. This lower amount of SI is associated to the lower interaction between the tool pin and the steel sheet, which is also affected by h. For this reason, the sample

of 146 mm/min, which has a higher h, showed a higher interaction and steel flow into Al sheet, with a consequently lower fracture load.

Related to the Ef, it must be considered that the thinning produced et al. sheet in the WN due to h and also by the hook affect the maximum value of Ef that it could be reached. This is especially relevant in thin sheets.

Figure 11 shows SEM images and EDS maps of Al and Fe of the fracture surface of the fractured lap shear test specimen for 146 mm/min.

The fracture surface shows two zones with different appearance (Fig. 11a). The upper zone presented a ductile fracture showing dimples with plastic deformation in shear (Fig. 11b) and only aluminium was detected on it (Fig. 11d). The lower zone presented a more brittle fracture (Fig. 11c) and both Fe and Al detected on it (Fig. 11e). The presence of both elements confirms that this zone corresponds to a SI.

This observation is consistent with what was observed previously, associated to the fracture path, confirming it follows the SI. Probably, the brittle fracture surface is associated to the IMC layer in the aluminium/steel interface between the aluminium matrix and the SI. Similar fractographies were obtained by Chen et al. (2013) for FSLW of dissimilar joints of aluminium alloy and steel (Chen et al. 2013).
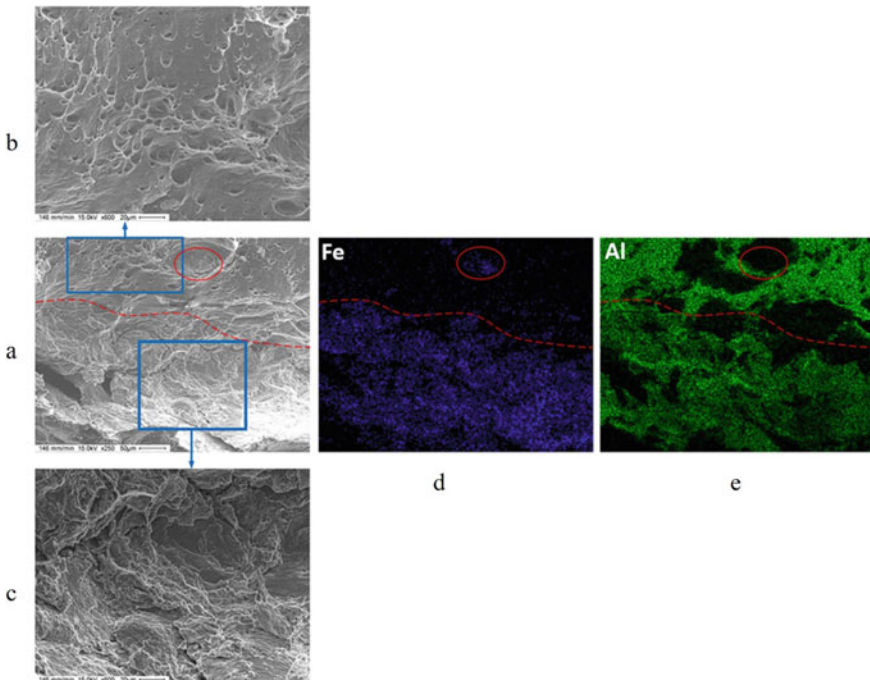
Fig. 11 SEM images and EDS mapping of Al and Fe of the fracture surface of the fractured lap shear test specimen for 146 mm/min

4 Conclusions

The effect of travel speed on mechanical properties and failure mechanism in dissimilar friction stir lap welding of AA5052-H32 and AISI 1010 in thin plates of 1 mm and 0.8 mm, respectively, was studied. The developed procedure showed to be adequate and could be qualify under ISO 25239, considering the scope of this standard.

Interaction between aluminium and steel was observed in the welding nugget, with the presence of steel inclusions in the aluminium welding nugget, especially in the hook zone, which decreased with travel speed. These steel inclusions increased the hardness of the AA5052 in the hook zone.

In lap shear test, interface showed a good integrity for all welding conditions. A tensile fracture mechanism was observed in all cases and the fracture was located at the P_{Hook}. Maximum load per unit width increased linearly with travel speed, reaching 73% of the tensile strength of the AA5052-H32 (for 206 mm/min).

On the fracture surface of tested samples there were identify two zones, one with a ductile fracture associated to the Al matrix, and the second with presence of Al and Fe, associated to the SI.

Steel inclusions in the welding nugget of the AA5052 controlled the fracture location, path and the maximum load per unit width.

To optimize the fracture load in this type of joints, the interaction between Al and Steel has to be high enough to produce an interface with good integrity but low enough to minimize the steel inclusions into the Al sheet thickness. This balance will lead to reach the maximum joint efficiency.

References

Beygi, R., Carbas, R.J.C., Barbosa, A.Q., Marques, E.A.S., da Silva, L.F.M.: A comprehensive analysis of a pseudo-brittle fracture at the interface of intermetallic of η and steel in aluminum/steel joints made by FSW: microstructure and fracture behavior. Mater. Sci. and Eng. A **824**, 141812 (2021). https://doi.org/10.1016/j.msea.2021.141812

Chen, Z.W., Yazdanian, S., Littlefair, G.: Effects of tool positioning on joint interface microstructure and fracture strength of friction stir lap Al-to-steel welds. J. Mater. Sci. **48**(6), 2624–2634 (2013). https://doi.org/10.1007/s10853-012-7056-0

Coelho, R.S., Kostka, A., Sheikhi, S., Dos Santos, J., Pyzalla, A.R.: Microstructure and mechanical properties of an AA6181-T4 aluminium alloy to HC340LA high strength steel friction stir overlap weld. Adv. Eng. Mater. **10**(10), 961–972 (2008). https://doi.org/10.1002/adem.200800028

Elrefaey, A., Gouda, M., Takahashi, M., Ikeuchi, K.: Characterization of aluminum/steel lap joint by friction stir welding. J. Mater. Eng. Perform. **14**(1), 10–17 (2005). https://doi.org/10.1361/10599490522310

International Organization for Standardization: Friction stir welding—aluminium—part 4: specification and qualification of welding procedures (ISO 25239-4:2011). ISO (2011). https://www.iso.org/

Kar, A., Vicharapu, B., Morisada, Y., Fujii, H.: Elucidation of interfacial microstructure and properties in friction stir lap welding of aluminium alloy and mild steel. Mater. Charact. 168, 110572 (2020). https://doi.org/10.1016/j.matchar.2020.110572

Kimapong, K., Watanabe, T.: Lap joint of A5083 aluminum alloy and SS400 steel by friction stir welding. Mater. Trans. JIM **46**(4), 835–841 (2005a). https://doi.org/10.2320/matertrans.46.835

Kimapong, K., Watanabe, T.: Effect of welding process parameters on mechanical property of FSW lap joint between aluminum alloy and steel. Mater. Trans. JIM **46**(10), 2211–2217 (2005b). https://doi.org/10.2320/matertrans.46.2211

Kumar, N., Yuan, W., Mishra, R.S.: Friction Stir Welding of Dissimilar Alloys and Materials. Butterworth-Heinemann, Oxford (2015)

Mishra, R.S., Mahoney, M.W. (ed.): Friction Stir Welding and Processing. ASM International, Ohio (2007)

Movahedi, M., Kokabi, A.H., Reihani, S.S., Najafi, H.: Mechanical and microstructural characterization of Al-5083/St-12 lap joints made by friction stir welding. J. Proc. Eng. **10**, 3297–3303 (2011). https://doi.org/10.1016/j.proeng.2011.04.544

Movahedi, M., Kokabi, A.H., Reihani, S.S., Najafi, H.: Effect of tool travel and rotation speeds on weld zone defects and joint strength of aluminium steel lap joints made by friction stir welding. Sci. Technol. Weld. Joining **17**(2), 162–167 (2012). https://doi.org/10.1179/1362171811Y.0000000092

Sorger, G., Wang, H., Vilaça, P., Santos, T.G.: FSW of aluminum AA5754 to steel DX54 with innovative overlap joint. Weld World **61**(2), 257–268 (2017). https://doi.org/10.1007/s40194-016-0412-y

Wan, L., Huang, Y.: Microstructure and mechanical properties of Al/Steel friction stir lap weld. Metals **7**(12), 542 (2017). https://doi.org/10.3390/met7120542